Overlapping of two truncated crisis scenarios: Generator of peaks in mean lifetimes of chaotic transients

Paar, Vladimir; Pavin, Nenad

Overlapping of two truncated crisis scenarios: Generator of peaks in mean lifetimes of chaotic transients

V. Paar* and N. Pavin

Department of Physics, Faculty of Science, University of Zagreb, Zagreb, Croatia
(Received 5 August 2002; revised manuscript received 25 March 2003; published 30 September 2003)

Maxima of mean transient time versus driving amplitude were found for weakly dissipated Duffing oscillator. In the neighborhood of peak of mean transient time an approximate power-law dependence was found. This behavior was compared with scaling in the vicinity of crisis point and interpreted as crossing of two neighboring crisis points which appears with decrease of driving amplitude. At this point chaotic attractor was destroyed and chaotic transient, exhibiting a maximum in the lifetime was borned. It was shown that the peak of mean lifetime has a regular behavior described by quadratic function.

I. INTRODUCTION

Transient chaotic behavior is common in the realm of nonlinear systems. Chaotic transient behaves chaotically during some transient time interval and then trajectory switches, often quite abruptly, into nonchaotic behavior [1–4]. The length of chaotic transient depends sensitively on initial conditions. However, if one takes many initial conditions, the chaotic transient lengths have an exponential distribution [5–8]

$$P(\tau) = \exp\left(-\frac{\tau}{\langle \tau \rangle}\right), \tag{1}$$

where $\langle \tau \rangle$ is the mean lifetime of the transient.

In global bifurcation category of routes to chaos, the chaotic transient route, referred to as crises [9,10], is the most important route for systems modeled by various sets of differential equations [1–4]. The crisis route to chaotic attractor is associated with collision of chaotic attractor and unstable periodic orbit or its stable manifold [1–4,9,10]. The common feature of such route are homoclinic and heteroclinic orbits which suddenly appear as the control parameter is varied and strongly influence the nature of other trajectories passing near them, as shown for example, for chaotic transients due to homoclinic and heteroclinic connections leading to chaotic behavior in the Lorenz model [3,11].

For a large class of dynamical systems which exhibit crisis, Grebogi, Ott, and Yorke [9,10] obtained the scaling of the mean lifetime $\langle \tau \rangle$ in the form

$$\langle \tau \rangle = \beta |p - p_c|^{-\gamma} \tag{2}$$

for the control parameter p close to the critical value p_c at which chaotic transient is replaced by chaotic attractor. Expressions for the critical exponent γ, which depend essentially on the stability properties of basic periodic orbit, were obtained as [12,13]

───────
*Electronic address: paar@hazu.hr

$$\gamma = \tfrac{1}{2} + (\ln|\alpha_1|)/|\ln|\alpha_2||, \tag{3}$$

in the case of heteroclinic tangency, and

$$\gamma = (\ln|\beta_1|)/(\ln|\beta_1\beta_2|^2), \tag{4}$$

in the case of homoclinic tangency, where $|\alpha_1|$, $|\beta_1|$, and $|\alpha_2|$, $|\beta_2|$ are expanding and contracting eigenvalues, respectively. In the case of unstable-unstable pair bifurcation crisis a faster increase of the characteristic scaling was obtained [12,13].

These phenomena have been studied mostly for nonlinear systems with sizeable dissipation.

In this paper we will investigate mean lifetimes of chaotic transients for the equation of a single-well Duffing oscillator:

$$\ddot{x} + d\dot{x} + x + x^3 = f \cos \omega t. \tag{5}$$

This equation was previously investigated in Ref. [14–16]. The system initially undergoes a period doubling subharmonic cascade that leads to chaos at $f = 23.0$ for $d = 0.1$ and $\omega = 0.95$. It quickly moves out of chaos with increasing f, and then goes back into chaotic oscillations at approximately $f = 32.0$.

II. SHRINKING OF CHAOTIC REGION BETWEEN TWO CRISIS POINTS

In this paper the system (5) was investigated for a sizeably lower dissipation ($d = 0.014$), keeping the driving frequency fixed at $\omega = 0.95$, and driving amplitude treated as control parameter.

An interesting pattern was obtained in the interval of f between $f = 23$ and $f = 32$, which was previously studied for sizeable dissipation. At $f = 23$ there is a chaotic attractor. Increasing the control parameter f, the system (5) passes through crisis. At critical value of control parameter $f = 23.08$ the chaotic attractor is destroyed. It is replaced by a chaotic repeller, invariant fractal set formed beyond the crisis [4]. Typical orbit beyond the crisis is transiently chaotic orbit, with well defined mean lifetime of chaotic transients $\langle \tau \rangle$ for a uniform set of initial conditions. Increasing the control parameter further, an inverse crisis scenario appears at f
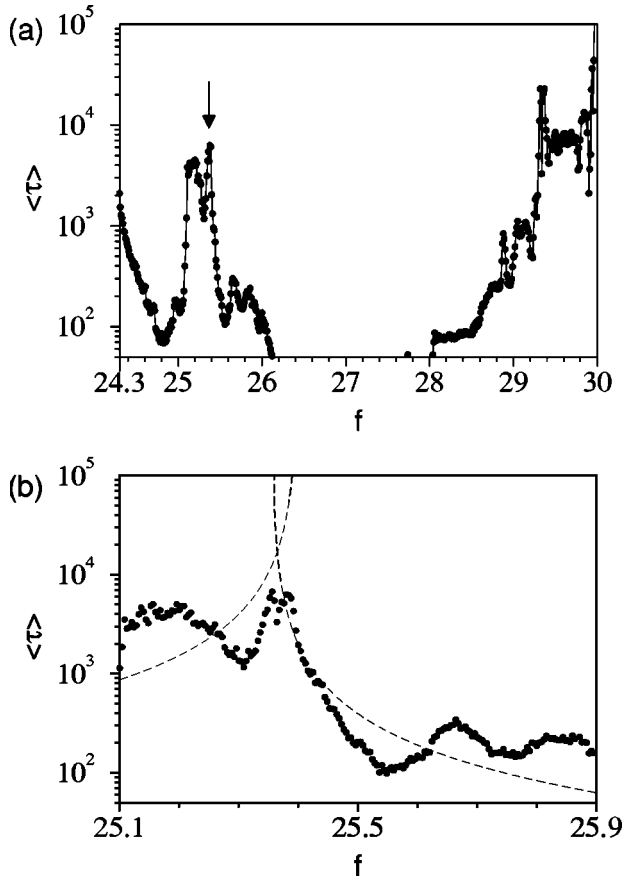
FIG. 1. (a) Mean lifetime $\langle\tau\rangle$ for control parameter f in the interval (24.3, 30.0) at dissipation $d=0.014$. Control parameter f is taken in steps of 0.1. Nature of the peak at $f\approx25.3$ denoted by an arrow was closely investigated. (b) Magnified section from $f=25.1$ to $f=25.9$ in (a). Dashed lines display an extrapolation of fits discussed in text.

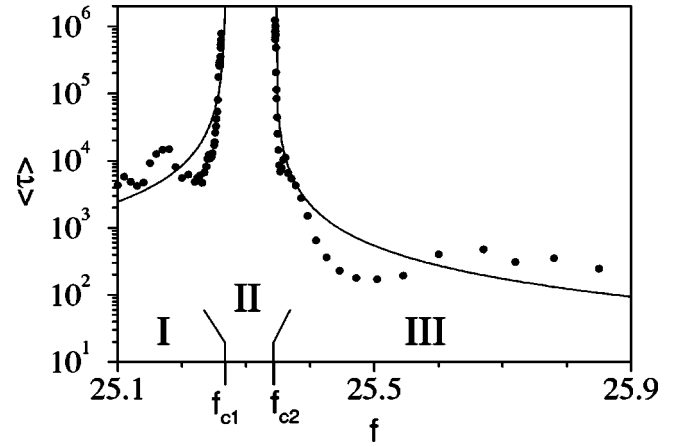

FIG. 2. Lifetimes of chaotic transient in the interval from $f=25.1$ to $f=25.9$ for $d=0.015$. Interval is segmented into three sections: chaotic transient (I), chaotic attractor (II), and chaotic transient (III). The two crisis points between the regions I and II, and II and III are denoted as f_{c1} and f_{c2}, respectively. For discussion see the text.

$=23.11$. At this crisis point the chaotic repeller is replaced by chaotic attractor, and the transiently chaotic orbits with well defined mean lifetime are replaced by stationary chaotic orbits (i.e., with lifetime $\langle\tau\rangle=\infty$). The whole interval between these two crisis points is characterized by transient chaos. Similarly, several additional crisis scenarios appear up to $f=32$.

Figure 1(a) displays mean lifetime of chaotic transients in the interval between $f=24.3$ and $f=30.0$ for weak dissipation $d=0.014$, expressed in terms of the period of driving force, $T=2\pi/\omega$. Immediately above the critical point at $f=24.3$ and below the inverse critical point at $f=30.0$, the mean lifetime of chaotic transient displays scaling behavior in accordance with the crisis scenario (2), decreasing from $\langle\tau\rangle=\infty$ at the crisis points. Between these two crisis points we found chaotic transient. However, further away from the crisis points in the interval between them, the lifetime of chaotic transient displays a complex dependence on the control parameter f, instead of smooth monotonic decrease. There are three pronounced peaks at $f=25.2$, $f=25.4$, and $f=29.3$. The peak at $f=25.4$ is magnified in Fig. 1(b).

Between these peaks, one observes pronounced minima at $f=24.8$ and $f\approx27$. The minimum at $f\approx27$ corresponds to the lifetime smaller than the relaxation times.

Let us discuss the origin of observed peaks in lifetimes. As already noted, dissipation in this study is much weaker than used in the previous studies of Duffing oscillator [14–16]. Therefore, it can be expected that the dependence of lifetime on the dissipation strength d will reveal the nature of this effect. From this point of view, we have performed the calculation for a slightly stronger dissipation, $d=0.015$, in the same interval of f as before (Fig. 2). Contrary to the situation in Fig. 1(b), for $d=0.015$ we find at the position of a peak at $f=25.3$ a narrow interval of chaotic attractor between $f_{c1}=25.268\,45$ and $f_{c2}=25.343\,89$ (interval II). The points denoted as f_{c1} and f_{c2} are the crisis points of onset and destruction of chaotic attractor in the narrow strip. Three intervals of f are shown in Fig. 2: region of transient chaos (25.1, 25.268 45) denoted I, region of chaotic attractor (25.268 45, 25.343 89) denoted II, and the region of transient chaos (25.343 89, 25.9) denoted III.

Here the transitions between the regions I and II, and between II and III can be recognized as two crisis points. These crises are due to collision of chaotic attractor and unstable periodic orbit of period-5. The value of critical exponent $\gamma_1=1.3774$ was calculated using Eq. (3) and the critical value of the control parameter f_{c1} was obtained according to procedure from Ref. [17]. Similar collision was observed at the crisis point f_{c2}. In that case $\gamma_2=1.3745$. For both crisis points Poincare surfaces are almost identical.

To get a better understanding of the origin of the peak, we have investigated geometrical shape of the attractor and stable manifold of the period-5 orbit. In transition from the region I into II (crisis point f_{c1}), the left arm of chaotic attractor is touching the stable manifold [Fig. 3(a)], i.e., the collision of attractor and manifold is in accordance with the crisis scenario. Increasing further the value of control parameter we enter into the region II. For a particular value of
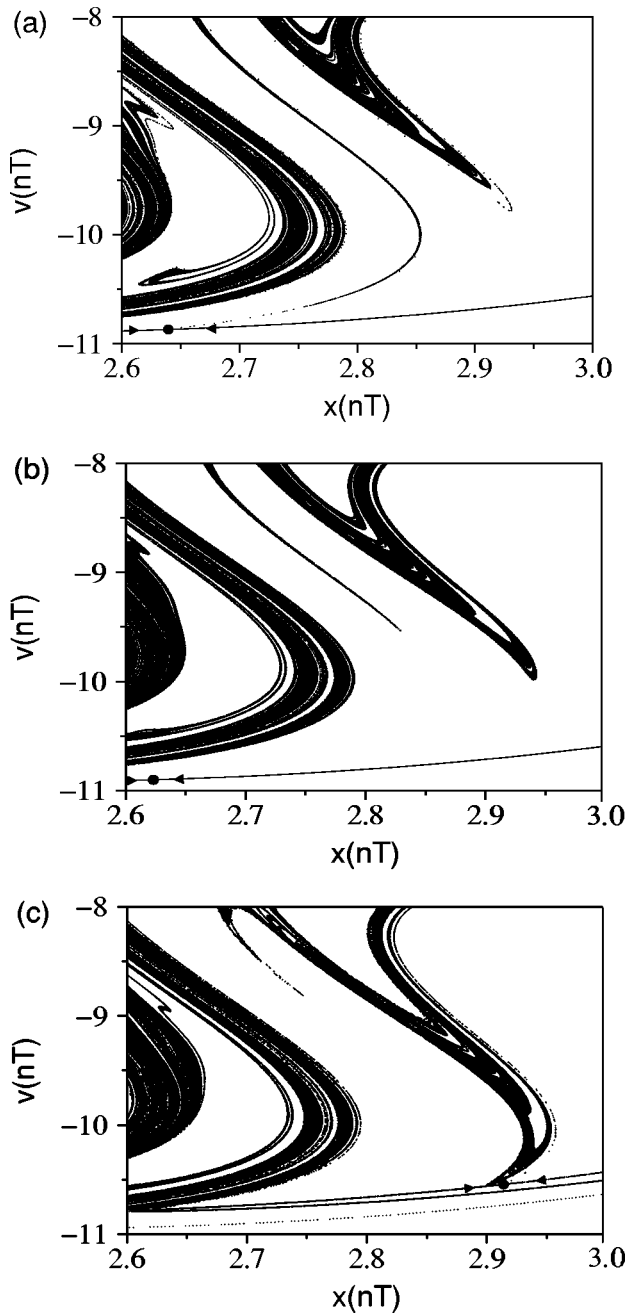
FIG. 4. Poincare sections displaying portion of chaotic attractor in collision with stable manifold of period-5 orbit at $f=f_{c1}=f_{c2}=25.349\,64$ at $d=0.014\,456$. Position of unstable period-5 orbit is marked by ●.

FIG. 3. Poincare sections displaying portion of chaotic attractor in collision with stable manifold of period-5 orbit. Position of the unstable period-5 orbit is marked by ●. (a) $f=f_{c1}$, (b) $f=25.3$, (c) $f=f_{c2}$ at $d=0.015$.

control parameter within the region II ($f=25.3$), the chaotic attractor and stable manifold are displayed [Fig. 3(b)]. This consideration reveals the nature of geometrical changes of chaotic attractor. With increase of control parameter the left arm of attractor (that has touched the unstable periodic orbit) is moving away from the stable manifold. Simultaneously, with increase of control parameter the right arm of attractor is approaching the stable manifold [Fig. 3(b)]. With a further increase of control parameter the right arm is approaching the stable manifold, and for $f=f_{c2}$ they collide [Fig. 3(c)].
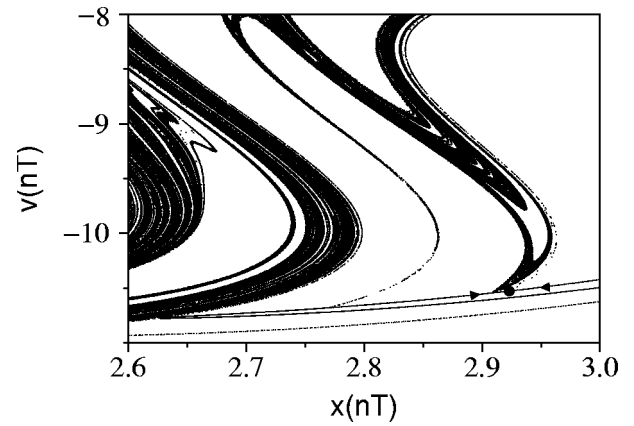
This collision can be recognized as transition from the region II into III, i.e., the crisis.

Lowering the dissipation strength d, the crisis points f_{c1} and f_{c2} are moving towards each other, i.e., the region II is narrowing. Particularly interesting is the value of dissipation strength associated with the collision of crisis points ($f_{c1}=f_{c2}$). In that moment, the region II disappears and we can state that the regions I and III are in collision. Numerically, we found that the collision of crisis points appears for $d=0.014\,456$. Figure 4 displays chaotic attractor and stable manifold at the point of touching ($f=f_{c1}=f_{c2}$). As seen, there is a simultaneous collision of the left and right arms of the attractor with the stable manifold.

For the control parameter f slightly smaller than $25.349\,64$ (Fig. 4), the left arm of the attractor collides with the stable manifold, resulting in destruction of attractor, in accordance with the crisis scenario. Similarly, for f slightly higher than $25.349\,64$, the right arm of attractor collides with stable manifold leading again to destruction of the attractor. Thus, the existence of chaotic attractor is associated with a particular value of control parameter. Additionally, we can argue that an additional lowering of dissipation can cause disappearance of chaotic attractor.

As seen from Fig. 3 the density of points differs in dependence on position on chaotic attractor. This density is decreasing with increase of Lyapunov exponent.

In the next step we performed the calculations of lifetimes for dissipation halfway between the two cases considered, i.e., for $d=0.0145$ (Fig. 5). In this case too, there is a narrow region of chaotic attractor, and the interval was segmented into three sections: I, II, and III. However, with respect to the previous case, the interval II of chaotic attractor is reduced. In particular, the crisis point $f_{c1}=25.333\,70$ has moved more towards higher values than the crisis point $f_{c2}=25.349\,15$.

We note that the calculated results exhibit fluctuations around the scaling curves. This is in accordance with general observation of fluctuations associated with crisis scenario [18,19].

As seen, small changes in dissipation strength d lead to small changes in the critical values of crisis points. Assum-
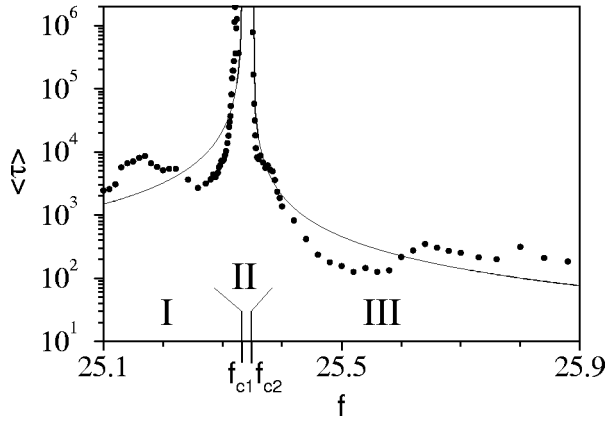
FIG. 5. Lifetimes of chaotic transient in the interval from f = 25.1 to f = 25.9 at dissipation d = 0.0145. For discussion see the text.
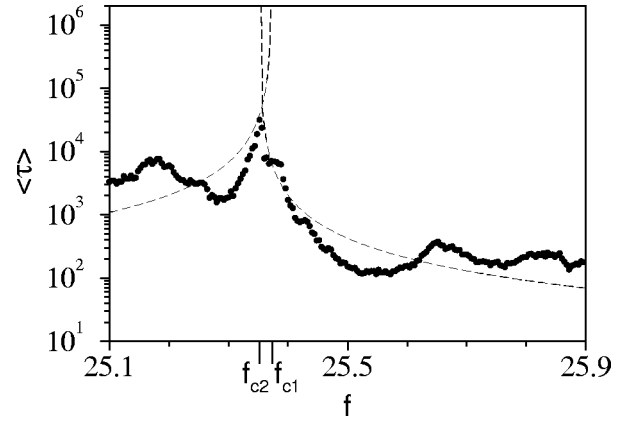

FIG. 6. Lifetimes of chaotic transient in the interval from f = 25.1 to f = 25.9 at dissipation d = 0.0142. Labels f_{c1} and f_{c2} are attributed on the basis of linear extrapolation. For discussion see the text.

ing linear extrapolation of positions of crisis points f_{c1} and f_{c2} to the first case of d = 0.014 where no chaotic attractor is present at $f \approx 25.3$, we have calculated the values of f_{c1}, f_{c2}, γ, and $\ln \beta$ (Table I). The corresponding curves are drawn in Fig. 1(b) (dashed lines). There is a crossing of two curves, i.e., of scaling corresponding to two crisis scenarios. At the position of crossing of two curves there is a maximum of lifetime in Fig. 1(b). This is more clearly seen from the calculations at d = 0.0142 (Fig. 6), which is still on the crossing side, but closer to the point of crossing. In accordance with the previous discussion the two crisis points are closer to each other and the crossing of two scaling curves gives a higher maximum, which will further increase towards the point of crossing. However, in Fig. 6 there is some difference of the shape of calculated peak in comparison to the shape of peak obtained by overlap of two scaling curves. Let us consider Fig. 6 taking into account that the change of dissipation leads to a shift of critical values f_{c1} and f_{c2}. As a starting point, let us assume that the change of dissipation leads to a shift of critical values, without any significant influence on the shape of curves. Accordingly, the values of lifetimes of chaotic transients from Fig. 5 (d = 0.0145) have been changed in such a way that the points appearing on the left-

hand side of the critical value f_{c1} were shifted to the right for Δf = 0.039 15, and the points on the right-hand side of f_{c2} to the right for Δf = 0.003 16. For d = 0.0142 the point f_{c1} has moved behind the point f_{c2}, the two curves in Fig. 5 have partially overlapped. For the points of overlap the lifetime of chaotic transients was calculated from the relation

$$\frac{1}{\langle \tau \rangle} = \frac{1}{\langle \tau_1 \rangle} + \frac{1}{\langle \tau_2 \rangle}, \qquad (6)$$

using values from both curves. Results obtained in this way are displayed in Fig. 7 (dashed line).

Let us more closely investigate the structure of the peak in the mean lifetime distribution, concerning the essential topic of this investigation.

Numerical procedure used in obtaining Figs. 6 and 7 shows a pattern which resembles at the first sight a singular structure. In order to clarify this issue a higher resolution computation was performed in the neighborhood of mean lifetime peak. To this end the resolution was increased
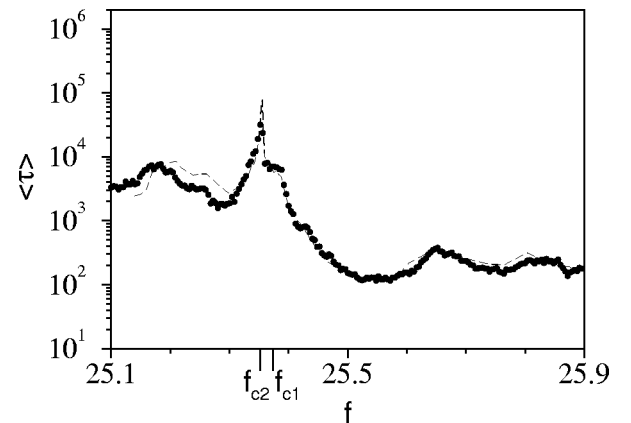
TABLE I. Critical values of control parameter f and of parameters β and γ in the power-law formula (2). For the first two rows the near-lying crisis parameters around f = 25.3 were used to determine parameters in the power-law formula (2). For dissipation d = 0.0140 and d = 0.0142 chaotic attractor at $f \approx 25.3$ disappears. The values given in the last two rows are determined by a straightforward linear extrapolation of the cases for d = 0.0150 and d = 0.0145.

d	f_{c1}	f_{c2}	γ_1	γ_2	$\ln \beta_1$	$\ln \beta_2$
0.0150	25.26845	25.34389	1.3774	1.3745	5.5	3.7
0.0145	25.33370	25.34915	1.3815	1.3809	5.3	3.5
0.0142	25.37285	25.35231	1.3840	1.3847	5.2	3.4
0.0140	25.39895	25.35441	1.3856	1.3873	5.1	3.3

FIG. 7. Lifetimes of chaotic transient in the interval from f = 25.1 to f = 25.9 at d = 0.0142. For discussion see the text.
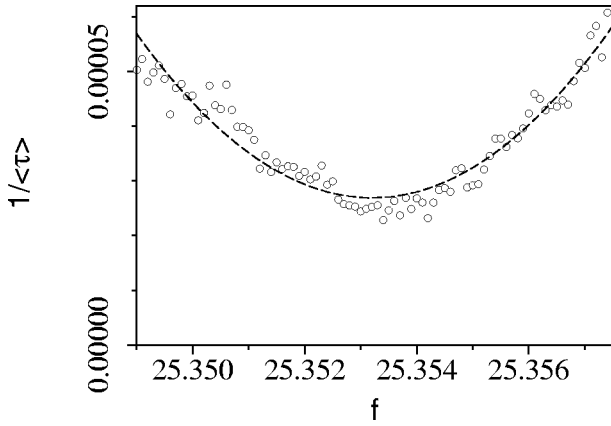
FIG. 8. Escape rate of chaotic transient $(1/\langle\tau\rangle)$ on lin-lin scale for interval of control parameter from $f=25.349$ to $f=25.3575$ with step $\Delta f=0.0001$ at dissipation $d=0.0142$. For discussion see the text.

20 times ($\Delta f=0.0001$). The results of calculation for the escape rate $1/\langle\tau\rangle$ was presented in Fig. 8. (The maximum of mean lifetime $\langle\tau\rangle$ corresponds to the minimum of escape rate $1/\langle\tau\rangle$.) From this higher resolution computation, it is evident that the pattern of the escape rate (i.e., of the mean lifetime) is in fact regular, with the presence of some local oscillations [18,19].

On the other hand, the use of Eq. (6) as an estimate for observed lifetimes would suggest that the peak displays a quadratic shape. Assuming that the approximate value of the escape rate is a superposition of two escape rates (6) and that the values $1/\langle\tau_1\rangle$ and $1/\langle\tau_2\rangle$ approximately satisfy the Grebogi-Ott-Yorke scaling (2), the total escape rate in the neighborhood of minimum value $(1/\langle\tau\rangle)_{min}$ was approximated by the second order Taylor expansion

$$\frac{1}{\langle\tau\rangle} \approx \left(\frac{1}{\langle\tau\rangle}\right)_{min} + \frac{1}{2}\left(\frac{1}{\langle\tau\rangle}\right)''_{f=f_0}(f-f_0)^2, \tag{7}$$

where

$$\left(\frac{1}{\langle\tau\rangle}\right)''_{f=f_0} = \frac{\gamma_1(\gamma_1-1)}{\beta_1}(f_{c1}-f_0)^{\gamma_1-2}$$

$$+ \frac{\gamma_2(\gamma_2-1)}{\beta_2}(f_0-f_{c2})^{\gamma_2-2}. \tag{8}$$

Here, f_0 denotes the value of control parameter f at which the escape rate achieves a minimum value $(1/\langle\tau\rangle)_{min}$.

Inserting into Eqs. (7) and (8) the parameter values from Table I for dissipation strength $d=0.0142$, we obtained

$$\frac{1}{\langle\tau\rangle} \approx 0.000\,025 + 1.7(f-25.3525)^2. \tag{9}$$

This theoretical prediction is rather close to the fit to the computed data in Fig. 8 (dashed line):

$$\frac{1}{\langle\tau\rangle} \approx 0.000\,027 + 1.7(f-25.3532)^2. \tag{10}$$

This leads to conclusion that the peak of mean lifetime has a regular (nonsingular) behavior which can be well represented by a quadratic function. A seemingly singular shape in Figs. 6 and 7 is a consequence of insufficient resolution because the quadratic maximum is not visible on the scale used in the figures.

III. CONCLUSION

For chaotic attractor in a narrow interval of control parameter, with crisis points at both ends, we have found in the same interval the appearance of a peak of lifetime of chaotic transient that is born with decreasing dissipation after destruction of chaotic attractor. This pattern, characteristic of weak dissipation, was explained in the framework of overlapping crisis scenarios, i.e., crossing of two end crisis points. It is noted that this may provide a mechanism for appearance of local maximum at each interval of chaotic attractor having crisis points at both ends, that is, shrinking with decreasing driving amplitude. The peak height is largest just following destruction of chaotic attractor and gradually decreases with further decrease of dissipation strength. Thus the interval with singularity $\langle\tau\rangle=\infty$ at dissipation strength above the value of control parameter corresponding to the crossing of two crisis points is replaced by a finite maximum. A general scheme of this effect is illustrated in Fig. 9. This mechanism can lead, in general, to multiple peaks in lifetime at weak dissipation. In the log-log plot these peaks are displayed as an approximate piecewise linear function, which can be interpreted in the framework of Grebogi-Ott-Yorke scaling.

To our knowledge, the pattern of multiple peaks in lifetime has not been reported so far in the literature, probably
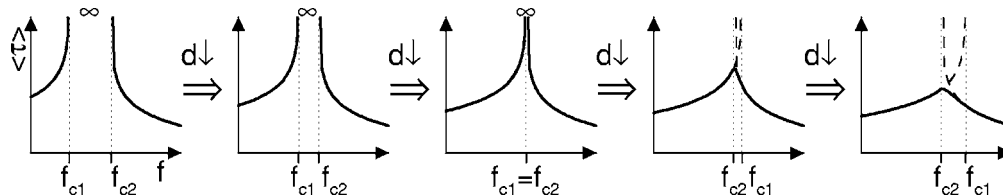

FIG. 9. Schematic presentation of crisis point crossing mechanism for generation of peaks in lifetime of chaotic transient with decreasing dissipation strength d.

because these peaks are associated with weak dissipation, while most of previous investigations have been performed at sizeable dissipation.

We have presented the pattern of peaks of lifetime for Duffing oscillator with linear dissipation, which is widely used as a model for studying nonlinear phenomena. In order to gain some additional evidence on possible generic nature of peaks of lifetime, we have additionally investigated a model with more complex Coulomb dissipation, containing the $\text{sgn}(\dot{x})$ and $\text{sgn}(\dot{x}^2)$ terms. Previously, bifurcation diagrams of that model have been investigated in Ref. [20]. Studying lifetimes of chaotic transients in that model, we found a qualitatively similar pattern of peaks as in the case of Duffing oscillator.

[1] E. Ott, *Chaos in Dynamical Systems* (Cambridge University Press, Cambridge, 1993).

[2] K. T. Alligood, T. D. Sauer, and J. A. Yorke, *Chaos* (Springer, New York, 1997).

[3] R. C. Hilborn, *Chaos and Nonlinear Dynamics* (Oxford University Press, Oxford, 1994).

[4] T. Tel, in *Direction in Chaos*, edited by Hao Bai-Lin (World Scientific, Singapore, 1990), Vol. 3, p. 149.

[5] J.A. Yorke and E.D. Yorke, J. Stat. Phys. **21**, 263 (1979).

[6] G. Pianigiani and J.A. Yorke, Trans. Am. Math. Soc. **252**, 351 (1979).

[7] H. Kantz and P. Grassberger, Physica D **17**, 75 (1985).

[8] K.Y. Tsang and M.A. Lieberman, Physica D **21**, 401 (1986).

[9] C. Grebogi, E. Ott, and J.A. Yorke, Phys. Rev. Lett. **48**, 1507 (1982).

[10] C. Grebogi, E. Ott, and J.A. Yorke, Physica D **7**, 181 (1983).

[11] E. A. Jackson, *Perspectives of Nonlinear Dynamics* (Cambridge University Press, New York, 1991), Vol. 2.

[12] C. Grebogi, E. Ott, and J.A. Yorke, Phys. Rev. Lett. **57**, 1284 (1986).

[13] C. Grebogi, E. Ott, F. Romeiras, and J.A. Yorke, Phys. Rev. A **36**, 5365 (1987).

[14] U. Parlitz and W. Lauterborn, Phys. Lett. **107A**, 351 (1985).

[15] Y. Ueda, Int. J. Non-Linear Mech. **20**, 481 (1985).

[16] C. Pezeshki and E.H. Dowell, Physica D **32**, 194 (1988).

[17] J.C. Sommerer and C. Grebogi, Int. J. Bifurcation Chaos Appl. Sci. Eng. **2**, 383 (1992).

[18] K. Kacperski and J.A. Holyst, Phys. Rev. E **60**, 403 (1999).

[19] K. Kacperski and J.A. Holyst, Phys. Lett. A **254**, 53 (1999).

[20] V. Paar, N. Pavin, N. Paar, and B. Novaković, Robotica **14**, 423 (1996); **18**, 201 (1998).